PYROLYSIS OF COMPLEXES OF METALLOSULPHOPHTHALOCYANINES WITH CHITOSAN FOR OBTAINING GRAPHITE-LIKE STRUCTURES

Natalia Sh. Lebedeva, Sabir S. Guseynov, Elena S. Yurina, Yury A. Gubarev, Anatoly I.

V'yugin

G.A. Krestov Institute of Solution Chemistry of the Russian Academy of Sciences,

Ivanovo, Russia, 153045

@*Corresponding author E-mail: gua@isc-ras.ru*

ORCID information:
Natalia Sh. Lebedeva **0000-0001-7260-3239**
Elena S. Yurina **0000-0002-2403-7049**
Yury A. Gubarev **0000-0003-2870-2189**

Abstract

The pyrolysis of chitosan and its polymeric complexes with metal phthalocyanines was studied by thermochemical and spectral methods. At all stages of thermal oxidation, the decomposition products of chitosan and polymer complexes with metal phthalocyanines were determined by the mass spectral method, the chemistry of the process was proposed. The pyrolysis of chitosan and its polymer complexes with metal sulphophthalocyanines leads to the formation of carbonizates with a wide variety of graphite-like structures with different contents of polyconjugated carbon-carbon bonds, the presence of which was confirmed by IR spectroscopy. It was shown that the introduction of copper(II)tetrasulphophthalocyanine into the composition of the polymer complex with chitosan results in an increase in the content of aliphatic structures in carbonizates, and the introduction of cobalt(II)tetrasulphophthalocyanine leads to aromatic compounds content increase. The possibility of changing the structures of chitosan carbonizates to obtain graphite-like structures by complexation with metal phthalocyanines has been shown.

Keywords

Pyrolysis, phthalocyanines, polymer, chitosan, carbonizates

Introduction

Chitosan is a natural polymer with great potential for structural chemical and physical modification. According to its chemical structure, chitosan is a linear aminopolysaccharide of 2-amino-2-deoxy-β-D-glucan being formed during deacetylation of chitin. The presence of reactive functional groups (OH and NH_2) in each structural unit of chitosan, a flexible structure of polymer chains and the ability to coordinate metal ions makes it possible to consider chitosan as a new functional biomaterial of high potential for its application in various fields. Being a hypoallergenic, biodegradable and biocompatible polymer with antimicrobial and antifungal characteristics, chitosan is widely used for biomedical purposes, as a blood anticoagulant, in drug delivery systems, in tissue engineering [1–5], as well as in other fields, such as wastewater treatment [6–8], food packaging [9,10], cosmetics [11], textile, paper and film technologies [12,13]. Recently, attempts have been made to study and develop technologies for producing carbon fibre from \chitosan [14,15]. The obtaining of carbon fibres from other polysaccharides includes the initial stage of thermal oxidation and exposure at a temperature of 300-400 °C, chemical and pyrolysis treatment [16]. However, carbon fibres obtained from cellulose and viscose are of unsatisfactory quality. It is considered that chitosan, due to its structural features, may be a more promising source of carbon fibres.

48 In this connection, the study of the processes occurring during the thermal and thermal
49 oxidative action on chitosan and its polymer complexes can help in improving industrial processes
50 planning and optimization.
51 This work is a continuation of earlier researches, in which the process of pyrolysis of a
52 wide range of chitosans and chitosan complexes (18.8 kDa, degree of deacetylation is 90.4%) with
53 sulphoderivatives of copper and cobalt phthalocyanines) was studied. As a result of it, the
54 temperature ranges of evaporation of physically and chemically bound water were revealed, and
55 thermal decomposition of chitosan and its complexes, the temperatures of physical and phase
56 transitions were established [17]. The introduction of sulphosubstituted phthalocyanines into the
57 polymer complex has nontrivial effects on the thermochemical behaviour of chitosan. It
58 conditioned the performing of thermogravimetric studies with synchronous recording of mass-
59 spectra in order to detail the chemical processes proceeding at various stages of chitosan pyrolysis
60 (18.8 kDa, degree of deacetylation is 90.4%) and of its complexes with sulphoderivatives of copper
61 and cobalt phthalocyanines). In addition, in that work, for these compounds information on thermal
62 oxidative destruction in the atmosphere of air was obtained The aim of this work is a comparative
63 analysis of the pyrolysis processes of chitosan and its complexes with metal phthalocyanines, as
64 well as a comparative analysis of the samples obtained by pyrolysis treatment of chitosan and its
65 complexes.
66
67 **Experimental part**
68 We used chitosan with a viscosity average molecular weight of 18 800 Da. The degree of
69 deacetylation of chitosan was determined by ^{1}H NMR spectroscopy described in [18]. ^{1}H NMR
70 spectra were recorded using Avance III (Bruker) (500.17 MHz) and 2% solution of DCl in D_2O as
71 a solvent for chitosan. The degree of deacetylation of the sample used in the work was 90.4 mol%.
72 Copper(II) (CuPc) and cobalt(II)tetrasulphophthalocyanines (CoPc) were synthesized and
73 purified according to the methods [19]. The purity of the tetrasulphophthalocyanines used in this
74 work was no less than 98%.
75 Crystalline samples of polymer complexes of chitosan with metal phthalocyanines were
76 obtained by evaporation of solutions with a sulphophthalocyanine concentration of $6.4 \cdot 10^{-5}$ M
77 and 0.02% chitosan.
78 Experimental studies of phase transitions and relaxation processes were carried out on a
79 DSC 204 F1 differential scanning heat flow calorimeter (Netzsch Gerätebau GmbH, Germany).
80 The test samples weighing 4-5 mg were placed in pressed aluminum crucibles with holes in the
81 cover. An empty aluminum crucible served as a reference sample. The calorimetric experiment
82 was carried out in a dynamic atmosphere of dry argon (argon content was 99.998%) with a gas
83 flow rate of 40 ml·min^{-1} and a heating rate of 10 °C·min^{-1}. All DSC measurements were made
84 relative to a baseline obtained for two empty crucibles. The temperature and sensitivity of the
85 calorimeter were calibrated by measuring the temperatures and enthalpies of phase transitions for
86 11 standard substances (Hg, C_6H_{12}, $C_{12}H_{10}$, KNO_3, $RbNO_3$, In, Bi, Sn, Zn, KClO4, CsCl). The
87 temperature measurement accuracy was 0.1 °C. The weighing accuracy was ± 0.001 mg
88 (Sartorius M2P balance).
89 Thermogravimetric analysis was carried out on a TG 209 F1 thermo-microbalance
90 (Netzsch Gerätebau GmbH, Germany). Powdered samples (4-7 mg) were placed into platinum
91 crucibles and heated at a rate of 10 °C·min^{-1} in a dynamic atmosphere of dry argon and air with a
92 gas flow rate of 30 ml·min^{-1} from room temperature to 600-700 °C. The accuracy of measuring
93 the sample mass was $1 \cdot 10^{-7}$ g.
94 Mass spectrometric analysis was performed using an STA 409CD thermoanalytical setup
95 (Netzsch Gerätebau GmbH, Germany) equipped with a mass spectrometer with a QMG 422
96 skimmer system (In Process Instruments, Germany), which made it possible to carry out
97 thermogravimetric and DSC measurements with synchronous registration of mass spectra of
98 thermal decomposition products. The samples were heated at atmospheric pressure in a flow of
99 dry ultrapure argon (70 ml·min^{-1}).

100   Scanning electron microscopy analysis of Microscopic images of the sample surfaces
101   were obtained with a VEGA 3 TESCAN scanning electron microscope (SEM) under vacuum
102   condition and at an accelerating voltage of 5.0 kV. Samples in the powder were placed on
103   aluminum butts.
104
105   **Discussion of the Results**
106   1. Pyrolysis
107   As noted above, we previously obtained thermochemical data reflecting the temperature
108   stages of pyrolysis of chitosan and its complexes with sulphophthalocyanines in an argon
109   atmosphere [17]. In continuation of the studies begun in order to establish the chemical processes
110   occurring at individual stages of pyrolysis, a combined thermal analysis was carried out with
111   synchronous registration of mass spectra of the samples under study in argon. Typical
112   temperature dependences of the curves (TG / DTG), DSC, and TIC (total ion current) for
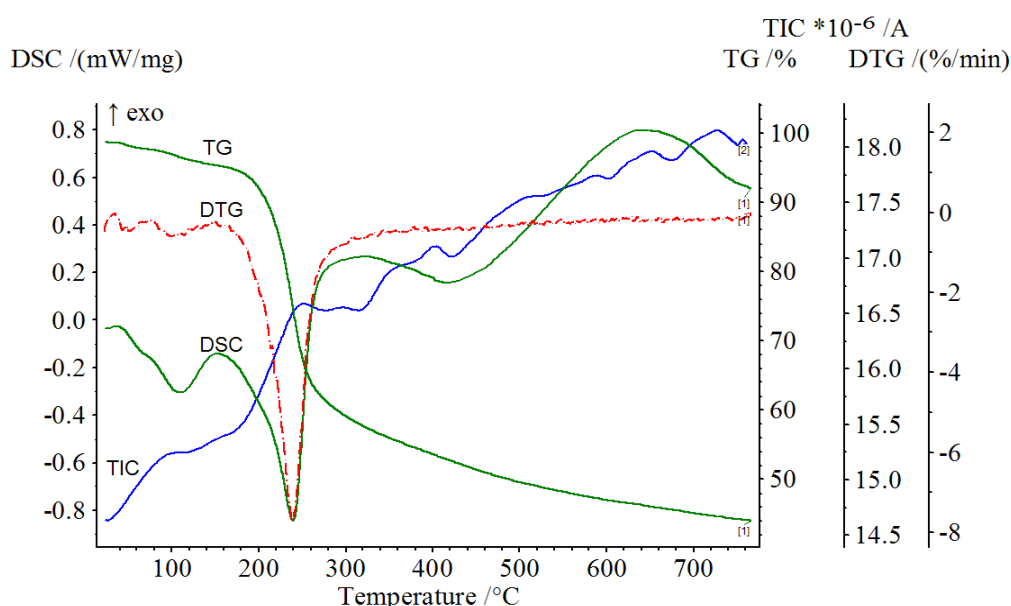113   chitosan in argon are shown in Figure 1.
114

115
116   **Figure 1.** TG/DTG/DSC/TIC curves obtained for degradation of CS at a heating rate of 10 ° C
117   min^{-1} in argon.
118
119   The mass numbers (m / z) of thermal decomposition products, the onset temperature
120   (Ton) and the temperature of the peak of the ion current intensity (Tmax) of the pyrolysis
121   process of CS, CSCoPc, and CSCuPc in the temperature range from 20 to 750 ° C are
122   summarized in Table 1.
123   The process of chitosan pyrolysis in argon is a multistage one (Figure 1). The first stage
124   (15-150 ° C) is accompanied by a weight loss on the TG curve of about 6 wt%, by an
125   endothermic peak on the DSC curve, and the removal of gaseous products with mass numbers m
126   / z = 18, 17 and 16, indicating the removal of water and its fragments. The maximum of this
127   process occurs at a temperature of 117 ° C (Table 1). Thus, the first stage consists in the removal
128   of physically and chemically sorbed water. A similar conclusion was reached by the authors [20]
129   who studied the IR spectra of chitosan samples heated to different temperatures.
130   The stage of chitosan dehydration partially overlaps with the beginning of its thermal
131   decomposition. The weight loss of the chitosan sample, according to TG data up to 320 °C, is 44
132   wt. %. The temperature of the maximum weight loss rate (Tmax) at this stage of thermal
133   decomposition of CS coincides with the endopeak on the DSC curve, indicating the predominance
134   of destructive processes. However. the asymmetric behaviour of the temperature dependence of
135   the DSC curve in the temperature range from 150 to 320 ℃, namely the transition of the unevenly
136   inclined endothermic peak to the exothermic peak, indicates both the destruction and the formation

3

137 of new chemical bonds in the test sample. Analysis of the mass spectra of thermal decomposition
138 products presented in Table 1 showed a complex pattern of chitosan pyrolysis, in which gaseous
139 products with mass numbers corresponding to fragments of H_2O, NH_3, CO, CO_2, HCl, and
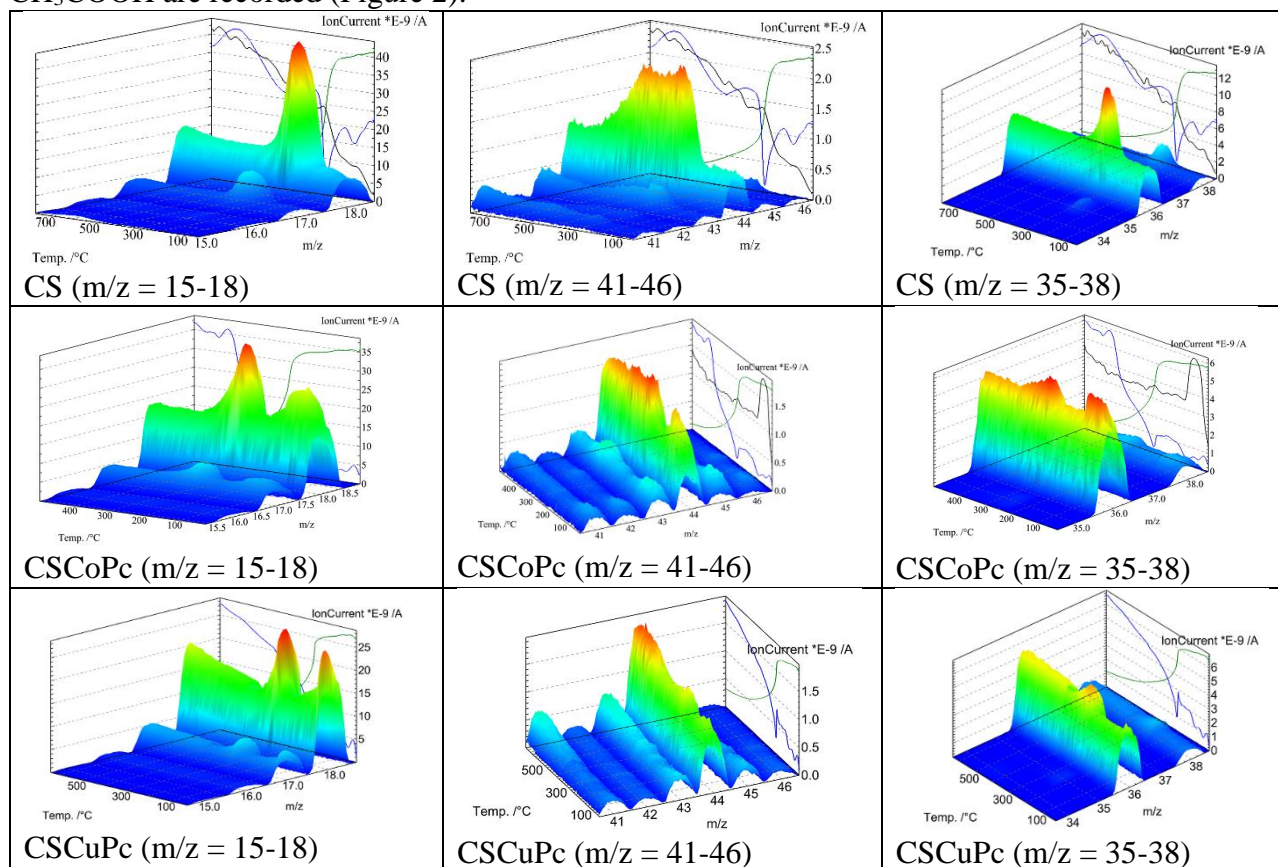140 CH_3COOH are recorded (Figure 2).

141
142 **Figure 2.** Mass spectra of gases evolved during the thermal treatment of CS, CSCoPc and
143 CSCuPc.

144
145   At the initial stage of destruction, upon reaching a temperature of 152-159 °C, the
146 formation of CO_2 is recorded (m / z = 44) (Table 1). The intensity of the ion current is
147 comparatively not high even at maximum emission, nevertheless, the event takes place. The
148 evolution of carbon dioxide, according to the literature [21,22], is attributed to an accidental
149 rupture of the C-O-C glycosidic bond, and the reaction products are shortened polymer chains,
150 oligomers, their radicals and CO_2.
151   Figure 2 shows that the maximum ionic current corresponds to the evolution of ammonia.
152 This process begins almost immediately (172-178 °C) after the dehydration stage, that is,
153 deamination processes dominate at the first stage of chitosan pyrolysis. We suppose that the
154 anomalous DSC curve of chitosan at this stage is due to the fact that the removal of NH_2 groups is
155 accompanied by crosslinking of fragments of the polymer chain or of adjacent macrochains
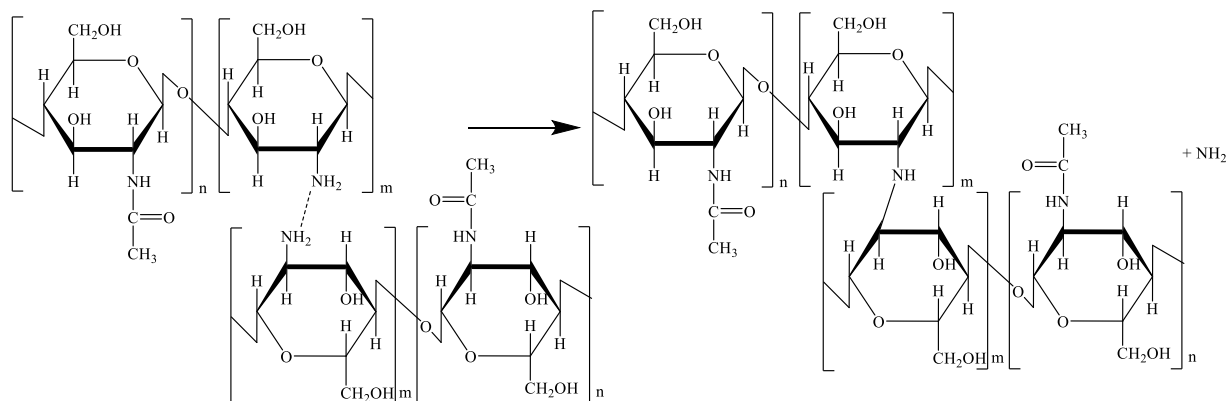156 (Figure 3).
157

158
159 **Figure 3.** Chitosan deamination reaction scheme
160 **Table 1.** Thermal degradation products of the CS, CSCoPc and CSCuPc.

products	m/z a.m.u	CS T_{on}, (°C)	CS T_{max}, (°C)	CSCoPc T_{on}, (°C)	CSCoPc T_{max}, (°C)	CSCuPc T_{on}, (°C)	CSCuPc T_{max}, (°C)
H_2O	18	55 172	117 244	37 171	70 227	35 170	69 217
H_2O H_2O, NH_3	17	55 172	117 244	37 171	70 227	35 170	69 217
CO_2	44	152-159 354	249 428	183 376	235 429	188 418	217 542-577
H_2O H_2O, NH_3 CH_4	16	55 172 411	117 248 585	37 171 389	70 227 434	35 164 393	65 217 563
Acetic acid	60	172-178	244	211	237	195-200	217-234
NH_3 CH_4	15	172-178 411	248 585	211 389	314 434	200 393	227 562
Acetic acid decomposition product	43	172-178	249	183	227-237	200	217-232
Acetic anhydride C_2H_2O, $(C_2H_4N^+)$	42	172-178	249	183	227-237	200	217-232
Acetaldehyde (CHO)	29	172	249	200	238	205	223
HCl	38	172	244	205	248	195	217-222
HCl	37	172	244	205	248	195	222
HCl	36	172	244	205	248	195	222
HCl	35	172	244	205	248	195	222
HCN	27	544	730	-	-	542	709
HCN	26	544	730	-	-	542	709
SO_2	64	-	-	217	299	269	408
SO_2	48	-	-	217	299	269	408

161
162   The formation of new structures is indirectly confirmed by the results of electron
163 microscopy of the initial chitosan samples and of the heated ones (Figure 4). It is seen that chitosan
164 heating (to 170 °C) leads to the formation of larger aggregates.
165   At the initial stage of chitosan pyrolysis, when the temperature reaches 172 °C, the
166 emission of acetic acid fragments (m / z = 15, 43, 60 [23]) and acetic anhydride (m / z = 42) is

recorded in the gas phase. Probably, the reaction of elimination of the side N-acetyl groups occurs (Figure 5).

In a number of works it was assumed that the products of the deacetylation reaction of chitosan can be polymer structures in which neighboring macrochains are connected at the site of cleavage of acetyl groups by bridging groups –N=N– or –NH–. We consider that with a high degree of chitosan deacetylation, as in this case (90.4%), the probability of macrochain crosslinking during deacetylation is low. Recently, many publications have appeared in the scientific literature [24–27], in which it was proposed to use the amount of the evolved acetic acid found in mass spectra to evaluate the degree of deacetylation. It should be noted that the formation of acetic acid from the acetyl groups of chitosan requires water (Figure 5); therefore, the results will depend on the course of dehydration reactions or on the residual water content in the polymer. One of such reactions, according to the authors [28], may be the reaction of the onset of destruction of pyrazine rings (T = 200 °C), in the course of which nitrogen- and oxygen-containing volatile compounds (furan and its derivatives, pyrazines and pyridines) can be formed. All the listed compounds in mass spectra have high m / z values, exceeding 67 units [26] and were not detected by us in the temperature range 150-320 °C in significant amounts. In addition, it is reliably known that the stage of destruction of monomeric units occurs after the cleavage of almost all glycosidic bonds in chitin and chitosan. This stage is high-temperature and occurs at temperatures above 250 °C [20,29]. Therefore, the reaction of intermolecular dehydration is more likely according to the scheme on Figure 6.

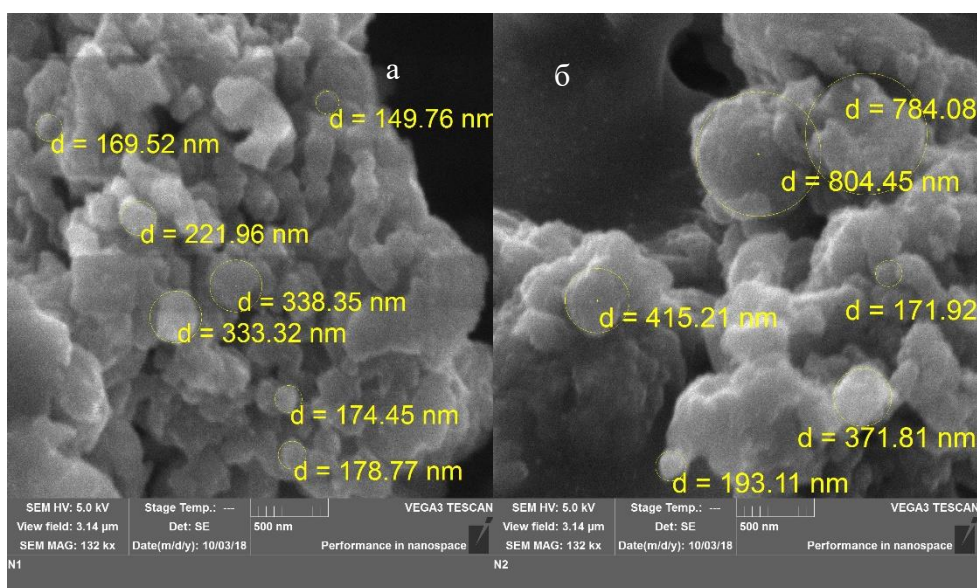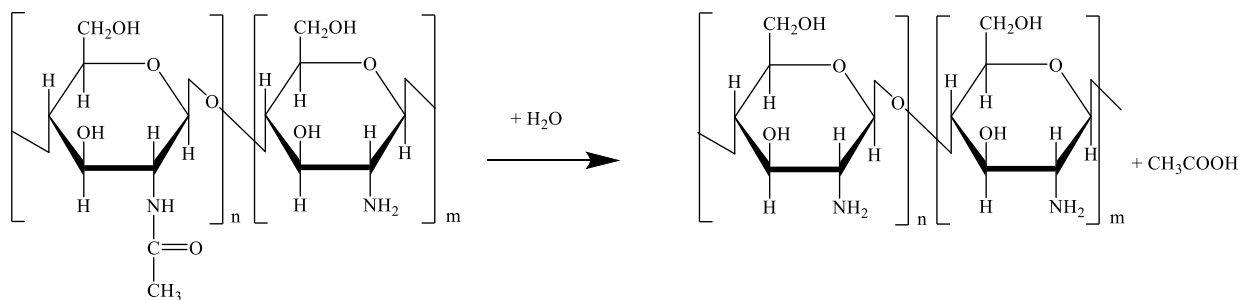**Figure 4.** Image of the structure of chitosan (a) before heating, (b) after heating to 170 °C.
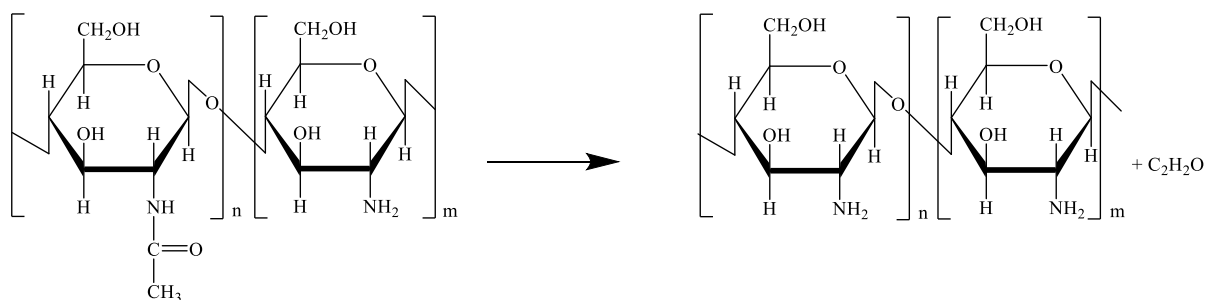

6

194
195 **Figure 5.** Schemes of chitosan deacetylation reactions.
196
197   In general, the pyrolysis of chitosan in the range of 150-320 °C is accompanied by a high
198 rate of the gaseous products removal with a weight loss, according to TG data, of about 44 wt. %.
199 Analysis of the mass spectra of the thermal decomposition products presented in Table 1 showed
200 a complex picture of the destruction of chitosan characterized by partially or completely
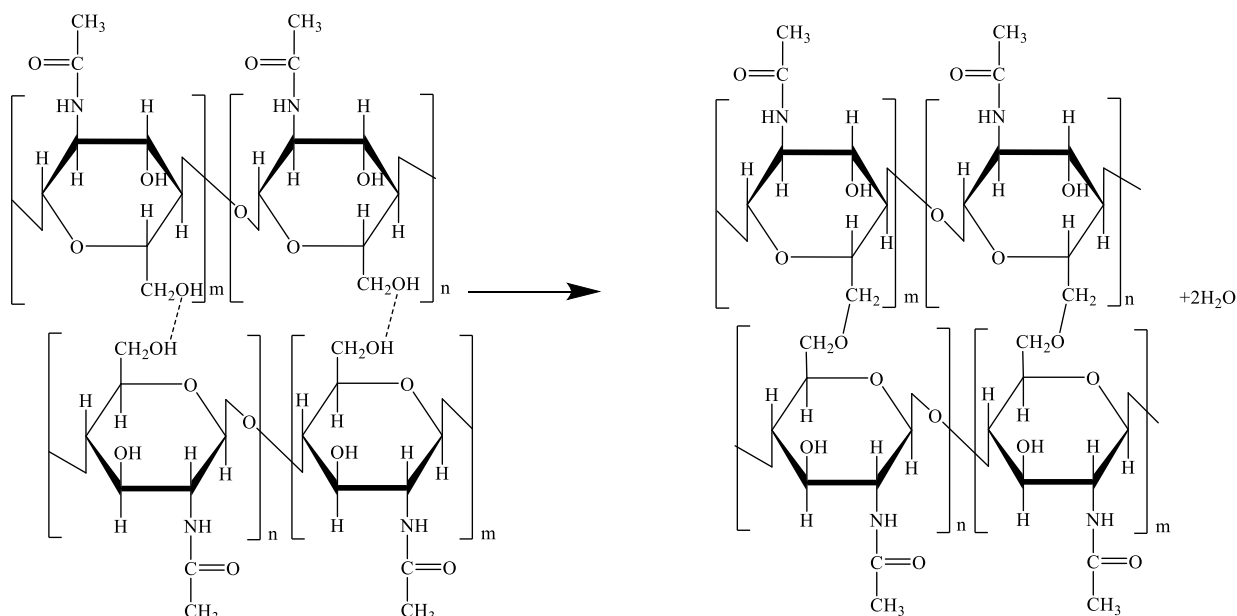201 overlapping steps.
202
203

204
205 **Figure 6.** Scheme of the dehydration reaction.
206
207   A further increase in temperature leads to the appearance of a pronounced exothermic
208 effect and a decrease in the rate of weight loss (Figure 1). The release of energy is usually
209 associated with the formation of new bonds. This exo-effect was observed earlier, but the
210 interpretation of this effect was different. For example, in [27] the exothermic effect with a
211 maximum at 310 °C is mainly attributed to the first stage of decomposition of the polysaccharide
212 - deacetylation, since it was found that the amount of energy released at this temperature increased
213 with an increase in the degree of deacetylation. A different opinion was uttered in the work [20]
214 which emphasizes that thermal degradation of chitosan occurs mainly by a free radical mechanism.
215 Intermediate radical products can spontaneously recombine, resulting in the formation of
216 crosslinked structures. The same opinion was shared by the authors [22] who proposed possible
217 schemes for the formation of crosslinked structures, the first stage of which is the break of the
218 glycosidic bond with the formation of radicals RO· and R· (R-fragment of the chitosan chain). The
219 author [21] adheres to a different position, considering that the exo-effect occurs due to the
220 formation of pyrazine and its derivatives as a result of complex condensation reactions of the
221 products of opening of pyrazine monomeric rings, Possible schemes for such reactions are
222 described in [29,30]. Probably, all of the above processes take place upon reaching 250 °C, when

223 the chitosan structure collapses. It should be noted that in this work pyrazine, pyridine, or furan
224 derivatives were not detected in significant amounts; the bulk of the weight loss was explained by
225 the processes involving the release of H_2O, NH_3, CO, CO_2, HCl, and CH_3COOH. These processes,
226 as noted above, begin at a temperature 172-178 °C and reach their maximum value at temperatures
227 of 244-249 °C.

228   Thus, the pyrolysis of chitosan begins with the simultaneous stages of deamination,
229 deacetylation, intermolecular dehydration, and to a lesser extent, there is a rupture of glycosidic
230 bonds. All these processes lead to the formation of crosslinked polymer structures even at
231 relatively low temperatures. Beginning from 220 °C, reactions occur with massive rupture of
232 glycosidic bonds (maximum emission of CO_2 is at 249 and 428 °C, Table 1) with the formation of
233 radical products, partial destruction of monomeric rings of pyrazine (with the formation of acetic
234 acid and ammonia, maximum emission at 244 °C, Table 1). The listed processes proceed
235 simultaneously with the recombination of radicals, leading to the formation of crosslinked polymer
236 structures that with a further increase in temperature up to 700 °C degrade without manifesting
237 bright effects (Figure 1). The main gaseous products at this stage are CO_2, CH_4, CHN. As can be
238 seen from Table 1, CO_2 emissions are two-stage. The second stage of CO_2 evolution begins at 354
239 °C and reaches a maximum at 428 °C. Along with this, there is a process characterized by the
240 release of CH_4, starting from 411 °C and reaching a maximum at 585 °C, as well as the release of
241 hydrogen cyanide CHN, with an onset temperature of 544 °C and a maximum of 730 °C. The
242 release of CH_4, CO_2, CHN suggests that further pyrolysis of the products formed after the first
243 stage of thermal decomposition of chitosan occurs, leading to the formation of products with a
244 high carbon content. The mass of the carbonizate obtained at 700 °C is about 46% of the initial
245 used chitosan.

246   The resulting carbonizate has been studied in the IR spectrum (Table 2). The latter turned
247 out to be very sparse, there were almost no infrared bands, only a band of medium intensity was
248 recorded at a frequency of 1610 cm^{-1} and a weak band of 804.5 cm^{-1}. Probably, graphite-like
249 structures were formed and they were characterized by the absence of IR spectra, since there were
250 no changes in the dipole moment when the atoms vibrated in a structure constructed from identical
251 carbon atoms [31]. It can be assumed that the detected absorption at 1610 cm^{-1} may be explained
252 by the valence vibrations of C=C in graphite-like structures or by vibrations of groups of C=O
253 conjugated with C-C atoms [32]. Absorption in the region at 1000-800 cm^{-1} is typical for C-C
254 groups that are part of unsaturated hydrocarbons or C-O-C valence vibrations of single-substituted
255 epoxides. Absorption in the area of 1100 -800 cm^{-1} is very wide and low-intensity, and these
256 parameters indicate a small polarity and a large variety of structures formed. The literature reports
257 on the composition of the carbonizate obtained under similar pyrolysis conditions. So, the authors
258 [14,33] discovered graphite-like structures in it. Moreover, as shown in [14], graphite-like
259 structures are formed from condensed aromatic carbon compounds. It should be noted that not
260 everything is so unambiguous - another work reported [20] that unsaturated and aromatic
261 hydrocarbons were not found in the carbonizate, but a structure typical for active carbon was
262 formed. Probably, the composition of the carbonizate significantly depends on the purity of the
263 initial chitosan and the presence of impurities affecting the initial stages of destruction.

264   A thermochemical study conducted earlier showed [17] that the formation of a chitosan
265 polymer complex with phthalocyanines leads to a slight decrease in the thermal stability of the
266 complexes. However, according to the data obtained (Table 1, Figure 7), the chemistry of the
267 pyrolysis process changes dramatically. In the context of this work, it is important to describe
268 briefly the information obtained earlier on the composition and structure of chitosan complexes
269 with the metal phthalocyanines. In our previous work, it was proved that chitosan binds
270 phthalocyanines differently [17,34]. CuPc in chitosan is in a dimerized state, the polymer complex
271 is formed due to electrostatic interactions between SO_3^--groups of metallophthalocyanine and NH^+
272 -groups of chitosan, H-binding of peripheral substituents of CuPc with the side groups of the CS
273 macrocycle, as well as due to hydrophobic forces. The CoPc in chitosan is in the monomeric state,
274 and the polymer complex is formed due to the donor-acceptor interaction between polymer

275 aminogroup of cobalt phthalocyanine atom, H-bonding of peripheral CoPc substituents to the side
276 groups of the CS macrochain, and, possibly, due to electrostatic interactions between the α-groups
277 of metallophthalocyanine and the β-groups of chitosan. The complexes, as in previous studies,
278 were obtained by mixing aqueous solutions of chitosan and the corresponding metal
279 phthalocyanines. The average composition of the polymer complexes is 1 MPc molecule:monomer
280 unit CS = 1:80.

281 As shown above, the process of complexation of chitosan with metal phthalocyanines is
282 not a classical chemical reaction, that is, the binding of MPc does not lead to chemical modification
283 of the polymer. Let us consider the effect of complexation of cobalt(II)- and
284 copper(II)phthalocyanines with chitosan on the chemistry of the pyrolysis process. The course of
285 the DSC curves of the CSCoPc and CSCuPc complexes significantly differs both from each other
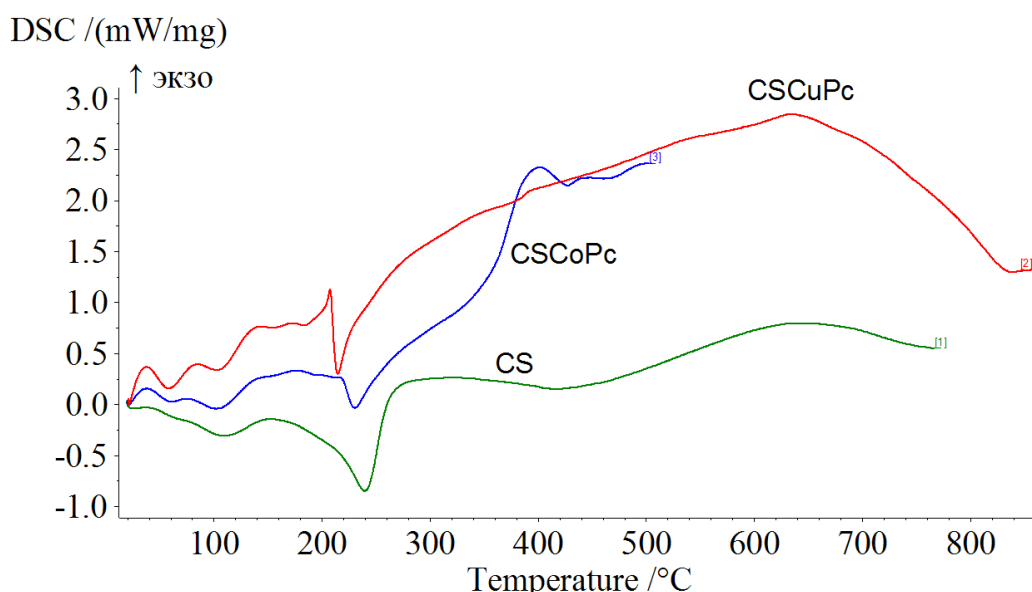286 and from CS (Figure 7); therefore, the chemistry of polymer pyrolysis also differs.
287

288
289
290 **Figure 7.** DSC curves obtained for degradation of CS, CSCoPc, CSCuPc at a heating rate of 10
291 °C·min^{-1} in argon.
292

293 Individual metal phthalocyanines are stable compounds, their degradation temperatures are
294 256 and 317 °C, respectively, and the thermal destruction itself begins with pyrolytic destruction
295 of sulphgroups, their maximum emission of products falls on 299 °C (CoPc) and 269 °C (CuPc)
296 (Table 1). Consequently, the initial stages of polymer destruction are not complicated by the
297 pyrolysis of metal phthalocyanines.
298 Judging by the value of the CO_2 emission current (m / z = 44), the probability of accidental
299 ruptures of glycosidic bonds in the composition of polymer complexes of chitosan with metal
300 phthalocyanines is even lower than in the case of individual chitosan (Table 1). In addition, the
301 temperature at which CO_2 is emitted is 30 °C higher in the complex than in pure chitosan (Table
302 1). Possibly, at the initial stage, metal phthalocyanines exhibit their antioxidant properties in the
303 composition of complexes with chitosan [35,36], inactivating randomly formed radicals and
304 thereby performing chain termination. Up to a certain temperature (183-188 °C) phthalocyanines
305 cope with the formed radicals.
306 As in the case of chitosan, at the initial stage of pyrolysis of CSCoPc complexes, CSCuPc
307 volatile products because of the deacetylation process. are recorded. Unlike chitosan, the emission
308 of fragments of acetic acid (m / z = 15, 43) and acetic anhydride (m / z = 42) in the case of
309 complexes CSCoPc and CSCuPc is recorded at higher temperatures: 183 C and 200 °C,
310 respectively, maximum emission is shifted in the range of low temperatures 227-237 °C (CSCoPc)

9

and 217-232 °C (CSCuPc). It should be noted that in the case of chitosan and CSCuPc deacetylation according to the scheme (Figure 5) proceeds in the same temperature range as the emission of fragments of N-acetyl groups, starting from 172 C and 200 °C, respectively (Table 1). On the contrary, in the case of CSCoPc, acetic acid is detected in mass spectra at a higher temperature, starting from 211 °C. Probably, in this case, acetic acid, like ammonia (Table 1), is formed as a result of decomposition of pyrazine rings.

The transition from chitosan to its complexes with metal phthlocyanines radically changes the chemical picture related to the release of ammonia (Figure 2). In the case of polymer complexes, the process becomes a two-step process. Starting from a temperature of 164 °C, the CSCuPc mass spectra record an ammonia signal which reaches its maximum at 217 and 227 °C (Table 1). It is noteworthy that starting at 180 ° C on the DSC CSCuPc curve, the process of ammonia release is accompanied by a rather pronounced exo-effect. We believe that the process proceeds according to scheme 3. Thus, the temperature of the onset of the deamination process in CSCuPc is 7 °C lower than in chitosan. A possible reason is the competitive interactions of phthalocyanine sulphogroups with the aminogroups of chitosan and the formed electrostatic and H-bonds of CuPc with chitosan, which weaken the C-N and N-H bonds.

In the case of CSCoPc, for which the main type of bond with chitosan is donor-acceptor interaction, the onset of the deamination process (Ton = 171 °C) practically coincides with the temperature set for chitosan, while the temperature of maximum NH$_3$ emission from the CSCoPc sample is lower by 17 °C. Another characteristic difference can be traced in the analysis of the DSC curve CSCoPc - in the analyzed temperature range the exo-effect is not recorded, probably, in this case the crosslinked polymer structures shown in Figure 3 are not formed. A possible reason may be steric hindrances created by CoPc for the formation of a network of hydrogen bonds between macrochains and screening of a part of aminogroups due to donor-acceptor interaction with CoPc. It is possible that it is these screened NH$_2$ groups that are split off with the maximum emission at a temperature of 314 °C (Table 1).

Attention is drawn to the fact that the temperature ranges Ton – Tmax get narrow in the presence of metal phthalocyanines; all the processes under consideration are much faster. It is obvious that the introduction of sufficiently bulky metal phthalocyanine molecules into the polymer disrupts the network of hydrogen bonds between macrocyclic chains, weakens the bonds and reduces the degree of crystallinity. All these structural changes in the polymer promote pyrolysis, facilitate the removal of volatile gaseous products, and, probably, contribute to the reaction rate increase.

Comparison of high-temperature processes occurring in the samples under study is problematic, since they are superimposed on the processes of destruction of peripheral substituents, and then of the macroring. However, it should be noted that, in general, the process of pyrolysis of CSCuPc is quite similar to the thermal destruction of chitosan, since, despite the high rate and change in the maximum temperatures, the composition of the volatile pyrolysis products is the same (Table 1). Complexation of chitosan with CoPc more significantly affects the chemistry of pyrolysis, leading to the disappearance, for example, of the low-temperature stage of the formation of cross-linked polymer structures, and the high-temperature stage associated with the emission of hydrogen cyanide.

Judging by the obtained IR spectra of carbonizates CSCuPc and CSCoPc, pyrolysis of polymer complexes of chitosan with phthalocyanines, all other things being equal, leads to the obtaining of somewhat different products. The spectra of carbonizates CSCuPc and CSCoPc, in contrast to the IR spectrum of chitosan carbonizate, contain a much larger number of the bands resolution (Table 2). As an example, Figure 8 shows the IR spectrum of CSCuPc and its carbonizate.

Table 2. IR spectra of carbonizates of chitosan and its complexes with copper(II) and cobalt(II) tetrasulfophthalocyanines.

Carbonizate

10

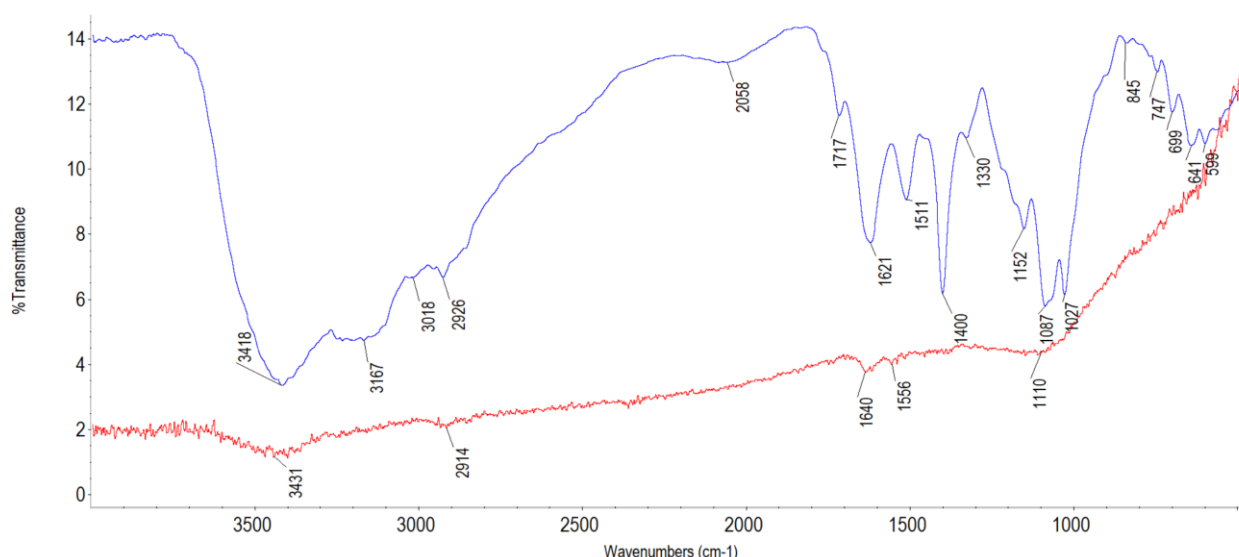| CS	CSCuPc	CSCoPc
570 wery weak	599 very weak	589 very weak
805 weak	-	874 very weak
-	1110 very int.	1131 broad, int.
-	1556 weak	-
1610 average	1639 average	1636 average
-	2914 weak	-
-	3432 broad, int.	3462

Figure 8. IR spectrum of the initial (upper line) and heated to 750 °C (lower line) CSCuPc.

The IR spectra of the carbonizates CSCuPc and CSCoPc are similar to each other, despite significant differences at the initial stage of pyrolysis. The 1640 cm^{-1} band, along with the 1200 - 1000 cm^{-1} bands, is referred to as aromatic compounds.

In addition, the band in the 1800-1600 cm^{-1} region, as noted above, may be due to the presence of C=O [32] groups.

Characteristic out-of-plane deformation vibrations of C-H in low-substituted aromatic compounds are manifested in the range of 670-900 cm^{-1} [31,32], and this phenomenon is observed in the case of carbonizate CSCoP. In the IR spectrum of CSCuPc this band is also visually detected, but it is much less intense. In this case, the IR spectrum of the carbonizate CSCuPc shows a band at about 1556 cm^{-1}, which most likely corresponds to the stretching vibrations of the C = C bond in olefins [37]. This assumption is also supported by the band at 2914 cm^{-1} associated with the stretching vibrations of the CH group in aliphatic compounds [32].

Noteworthy is the presence in the IR spectra of carbonizates CSCuPc and CSCoPc of a very wide band in the region of 3400 cm^{-1},probably, due to the presence of terminal OH groups of carbohydrates; moreover, the band in the region of 1140-1100 cm^{-1} can also refer to the vibrations of the valence bond C-O fragment of carbohydrates C-OH [32,38].

Thus, the pyrolysis of chitosan and its polymeric complexes with metal sulphothalocyanines leads to the formation of carbonizates with a wide variety of graphite-like structures with different content of polyconjugated carbon-carbon bonds. The introduction of CuPc causes an increase in the content of aliphatic structures, and CoPc - of aromatic compounds. In conclusion, we would like to note that the pyrolysis of chitosan and its polymer complexes can probably become a valuable tool for obtaining graphite-like structures.

Acknowlegements

11

References

[1]	B. Sarmento, J. Das Neves, Chitosan-Based Systems for Biopharmaceuticals: Delivery, Targeting and Polymer Therapeutics, 2012. https://doi.org/10.1002/9781119962977.

[2]	M.N.V.R. Kumar, R.A.A. Muzzarelli, C. Muzzarelli, H. Sashiwa, A.J. Domb, Chitosan chemistry and pharmaceutical perspectives, Chem. Rev. (2004). https://doi.org/10.1021/cr030441b.

[3]	S.A. Agnihotri, N.N. Mallikarjuna, T.M. Aminabhavi, Recent advances on chitosan-based micro- and nanoparticles in drug delivery, J. Control. Release. (2004). https://doi.org/10.1016/j.jconrel.2004.08.010.

[4]	R. Riva, H. Ragelle, A. Des Rieux, N. Duhem, C. Jérôme, V. Préat, Chitosan and chitosan derivatives in drug delivery and tissue engineering, Adv. Polym. Sci. (2011). https://doi.org/10.1007/12_2011_137.

[5]	G. Kratz, C. Arnander, J. Swedenborg, M. Back, C. Falk, I. Gouda, O. Larm, Heparin-chitosan complexes stimulate wound healing in human skin, Scand. J. Plast. Reconstr. Surg. Hand Surg. (1997). https://doi.org/10.3109/02844319709085478.

[6]	R. Yang, H. Li, M. Huang, H. Yang, A. Li, A review on chitosan-based flocculants and their applications in water treatment, Water Res. (2016). https://doi.org/10.1016/j.watres.2016.02.068.

[7]	Y. Liu, Y. Li, J. Lv, G. Wu, J. Li, Graft copolymerization of methyl methacrylate onto chitosan initiated by potassium ditelluratocuprate(III), J. Macromol. Sci. - Pure Appl. Chem. (2005). https://doi.org/10.1080/10601320500189414.

[8]	A. El-Shafei, S. Shaarawy, A. Hebeish, Graft copolymerization of chitosan with butyl acrylate and application of the copolymers to cotton fabric, Polym. - Plast. Technol. Eng. (2005). https://doi.org/10.1080/03602550500207840.

[9]	H.K. No, S.P. Meyers, W. Prinyawiwatkul, Z. Xu, Applications of chitosan for improvement of quality and shelf life of foods: A review, J. Food Sci. (2007). https://doi.org/10.1111/j.1750-3841.2007.00383.x.

[10]	P.K. Dutta, S. Tripathi, G.K. Mehrotra, J. Dutta, Perspectives for chitosan based antimicrobial films in food applications, Food Chem. (2009). https://doi.org/10.1016/j.foodchem.2008.11.047.

[11]	I. Aranaz, N. Acosta, C. Civera, B. Elorza, J. Mingo, C. Castro, M. de los L. Gandía, A.H. Caballero, Cosmetics and cosmeceutical applications of chitin, chitosan and their derivatives, Polymers (Basel). (2018). https://doi.org/10.3390/polym10020213.

[12]	S.H. Lim, S.M. Hudson, Review of chitosan and its derivatives as antimicrobial agents and their uses as textile chemicals, J. Macromol. Sci. - Polym. Rev. (2003). https://doi.org/10.1081/MC-120020161.

[13]	C.K.S. Pillai, W. Paul, C.P. Sharma, Chitin and chitosan polymers: Chemistry, solubility and fiber formation, Prog. Polym. Sci. (2009). https://doi.org/10.1016/j.progpolymsci.2009.04.001.

[14]	M. Bengisu, E. Yilmaz, Oxidation and pyrolysis of chitosan as a route for carbon fiber derivation, Carbohydr. Polym. (2002). https://doi.org/10.1016/S0144-8617(02)00018-8.

[15]	M.N.V. Ravi Kumar, A review of chitin and chitosan applications, React. Funct. Polym. (2000). https://doi.org/10.1016/S1381-5148(00)00038-9.

[16]	G. Savage, G. Savage, The Properties of Carbon-carbon Composites, in: Carbon-Carbon Compos., 1993. https://doi.org/10.1007/978-94-011-1586-5_8.

[17]	N.S. Lebedeva, S.S. Guseinov, E.S. Yurina, Y.A. Gubarev, O.I. Koifman, Thermochemical research of chitosan complexes with sulfonated metallophthalocyanines,

444   Int. J. Biol. Macromol. (2019). https://doi.org/10.1016/j.ijbiomac.2019.07.051.

445   [18]   A. Hirai, H. Odani, A. Nakajima, Determination of degree of deacetylation of chitosan by
446   1H NMR spectroscopy, Polym. Bull. (1991). https://doi.org/10.1007/BF00299352.

447   [19]   G.P. Shaposhnikov, V.P. Kulinich, V.E. Maizlish, Modifitsirovannye ftalotsianiny i ikh
448   strukturnye analogi, Liq. Cryst. Their Appl. Moscow Krasand. (2012).

449   [20]   J. Zawadzki, H. Kaczmarek, Thermal treatment of chitosan in various conditions,
450   Carbohydr. Polym. (2010). https://doi.org/10.1016/j.carbpol.2009.11.037.

451   [21]   C. Ou, S. Chen, Y. Liu, J. Shao, S. Li, T. Fu, W. Fan, H. Zheng, Q. Lu, X. Bi, Study on
452   the thermal degradation kinetics and pyrolysis characteristics of chitosan-Zn complex, J.
453   Anal. Appl. Pyrolysis. (2016). https://doi.org/10.1016/j.jaap.2016.03.021.

454   [22]   M. Mucha, A. Pawlak, Complex study on chitosan degradability, Polimery/Polymers.
455   (2002). https://doi.org/10.14314/polimery.2002.509.

456   [23]   Y.S. Nam, W.H. Park, D. Ihm, S.M. Hudson, Effect of the degree of deacetylation on the
457   thermal decomposition of chitin and chitosan nanofibers, Carbohydr. Polym. (2010).
458   https://doi.org/10.1016/j.carbpol.2009.11.030.

459   [24]   G.S. Lal, E.R. Hayes, Determination of the amine content of chitosan by pyrolysis-gas
460   chromatography, J. Anal. Appl. Pyrolysis. (1984). https://doi.org/10.1016/0165-
461   2370(84)80012-1.

462   [25]   J. Mattai, E.R. Hayes, Characterization of chitosan by pyrolysis-mass spectrometry, J.
463   Anal. Appl. Pyrolysis. (1982). https://doi.org/10.1016/0165-2370(82)80019-3.

464   [26]   H. Sato, S. Mizutani, S. Tsuge, H. Ohtani, K. Aoi, A. Takasu, M. Okada, S. Kobayashi, T.
465   Kiyosada, S. Shoda, Determination of the degree of acetylation of chitin/chitosan by
466   pyrolysis-gas chromatography in the presence of oxalic acid, Anal. Chem. 70 (1998) 7–
467   12.

468   [27]   J.M. Nieto, C. Peniche-Covas, G. Padro´n, Characterization of chitosan by pyrolysis-mass
469   spectrometry, thermal analysis and differential scanning calorimetry, Thermochim. Acta.
470   (1991). https://doi.org/10.1016/0040-6031(91)80260-P.

471   [28]   C. Peniche-Covas, W. Argüelles-Monal, J. San Román, A kinetic study of the thermal
472   degradation of chitosan and a mercaptan derivative of chitosan, Polym. Degrad. Stab.
473   (1993). https://doi.org/10.1016/0141-3910(93)90120-8.

474   [29]   L. Zeng, C. Qin, L. Wang, W. Li, Volatile compounds formed from the pyrolysis of
475   chitosan, Carbohydr. Polym. (2011). https://doi.org/10.1016/j.carbpol.2010.10.007.

476   [30]   P.-S. Wang, G. V Odell, Formation of pyrazines from thermal treatment of some amino-
477   hydroxy compounds, J. Agric. Food Chem. 21 (1973) 868–870.

478   [31]   V. Gomez-Serrano, J. Pastor-Villegas, A. Perez-Florindo, C. Duran-Valle, C. Valenzuela-
479   Calahorro, FT-IR study of rockrose and of char and activated carbon, J. Anal. Appl.
480   Pyrolysis. (1996). https://doi.org/10.1016/0165-2370(95)00921-3.

481   [32]   B.C. Smith, Fundamentals of fourier transform infrared spectroscopy, second edition,
482   2011.

483   [33]   H. Kaczmarek, J. Zawadzki, Chitosan pyrolysis and adsorption properties of chitosan and
484   its carbonizate, Carbohydr. Res. (2010). https://doi.org/10.1016/j.carres.2010.02.024.

485   [34]   N.S. Lebedeva, Y.A. Gubarev, E.S. Yurina, A.I. Vyugin, I.M. Lipatova, Features of
486   chitosan interaction with copper(II) and cobalt(II) tetrasulfophthalocyanines, Russ. J. Gen.
487   Chem. 87 (2017). https://doi.org/10.1134/S1070363217100139.

488   [35]   G.P. Amaral, G.O. Puntel, C.L. Dalla Corte, F. Dobrachinski, R.P. Barcelos, L.L. Bastos,
489   D.S. Ávila, J.B.T. Rocha, E.O. Da Silva, R.L. Puntel, F.A.A. Soares, The antioxidant
490   properties of different phthalocyanines, Toxicol. Vitr. (2012).
491   https://doi.org/10.1016/j.tiv.2011.10.006.

492   [36]   C. Kantar, H. Akal, B. Kaya, F. Islamoꞡlu, M. Türk, S. Şaşmaz, Novel phthalocyanines
493   containing resorcinol azo dyes; Synthesis, determination of pKa values, antioxidant,
494   antibacterial and anticancer activity, J. Organomet. Chem. (2015).
495   https://doi.org/10.1016/j.jorganchem.2014.12.042.

496   [37]   E. Fuente, J.A. Menéndez, M.A. Díez, D. Suárez, M.A. Montes-Morán, Infrared
497   spectroscopy of carbon materials: A quantum chemical study of model compounds, J.
498   Phys. Chem. B. (2003). https://doi.org/10.1021/jp027482g.
499   [38]   W.W. Duley, D.A. Williams, The infrared spectrum of interstellar dust: Surface functional
500   groups on carbon, Mon. Not. R. Astron. Soc. (1981).
501   https://doi.org/10.1093/mnras/196.2.269.
502